

# An AM1 theoretical study on the effect of $Zn^{2+}$ Lewis acid catalysis on the mechanism of the cycloaddition between 3-phenyl-1-(2-pyridyl)-2-propen-1-one and cyclopentadiene

C. N. Alves,<sup>a,b</sup> A. B. F. da Silva,<sup>a,\*</sup> S. Martí,<sup>c</sup> V. Moliner,<sup>c</sup> M. Oliva,<sup>c</sup> J. Andrés<sup>c</sup>  
and L. R. Domingo<sup>d</sup>

<sup>a</sup>Departamento de Química e Física Molecular, Instituto de Química de São Carlos, Universidade de São Paulo, CP 780, 13560-970 São Carlos, SP, Brazil

<sup>b</sup>Departamento de Química, Centro de Ciências Exatas e Naturais, Universidade Federal do Pará, CP 11101, 66075-110 Belém, PA, Brazil

<sup>c</sup>Departament de Ciències Experimentals, Universitat Jaume I, Box 224, 12080 Castelló, Spain

<sup>d</sup>Departamento de Química Orgánica, Universidad de Valencia, Dr. Moliner 50, 46100 Burjassot, Valencia, Spain

Received 9 October 2001; accepted 14 January 2002

**Abstract**—The mechanism of the Diels–Alder reaction between 3-phenyl-1-(2-pyridyl)-2-propen-1-one and cyclopentadiene has been investigated with the AM1 semiempirical method. Stationary points for two reactive channels, *endo-cis* and *exo-cis*, have been characterized. The role of the Lewis acid catalyst has been modeled taking into account the formation of a complex between  $Zn^{2+}$  and the carbonyl oxygen atom and the pyridyl nitrogen atom of the 3-phenyl-1-(2-pyridyl)-2-propen-1-one system with and without the presence of two molecules of water around the cation. The mechanism of the uncatalyzed reaction corresponds to a concerted process, but in the presence of Lewis acid catalyst the mechanism changes and the reaction takes place through a stepwise mechanism. A first step involves the nucleophilic attack of the cyclopentadiene in the double bond of the dienophile which produces an intermediate. A second step involves the closure of the intermediate yielding the corresponding final cycloadduct. The inclusion of the  $Zn^{2+}$  catalyst drastically decreases the energy barrier associated with the carbon–carbon bond formation of the first step in comparison to the concerted process. © 2002 Elsevier Science Ltd. All rights reserved.

## 1. Introduction

The Diels–Alder reaction is a powerful tool employed frequently in the synthesis of six-membered ring systems with excellent stereoselective control.<sup>1</sup> The remarkable importance of Diels–Alder reactions in the synthesis of natural products and physiologically active molecules led to the development of new methods to study [4+2] cycloaddition reactions.<sup>1</sup>

The study made by Yates and Eaton,<sup>2</sup> in which was showed that  $AlCl_3$  strongly accelerates the Diels–Alder reaction (both related to proton catalysis and thermal conditions), encouraged the development of Diels–Alder cycloaddition reactions of poorly reactive dienophiles<sup>3</sup> and several other carbon–carbon bond-forming reactions.<sup>4</sup>

Recent experimental studies on the rate and *endo–exo* selectivity of Diels–Alder reactions between different bidentate

dienophiles have been extensively investigated by Engberts et al.<sup>5</sup> These authors studied the effects of  $Co^{2+}$ ,  $Ni^{2+}$ ,  $Cu^{2+}$ , and  $Zn^{2+}$  ions, as Lewis acid catalysts, on the rate and *endo–exo* diastereoselectivity of Diels–Alder reactions between the bidentate 3-phenyl-1-(2'-pyridyl)-2-propen-1-one (R1) and cyclopentadiene (CP)<sup>5b</sup> (Fig. 1). These experimental studies have offered the possibility of carrying out a complementary theoretical analysis in order to attain a better interplay between theory and experiment.

We have recently studied the reaction between (*E*)-methyl cinnamate and cyclopentadiene in the presence of  $BF_3$ ,  $AlCl_3$ , and catechol boron bromide.<sup>6</sup> In that study we observed that the reaction mechanism changes in the presence of catechol boron bromide and the reaction takes place along a stepwise mechanism.<sup>6</sup> Tanaka and Kanemasa<sup>7</sup> have studied the cycloaddition reaction between nitron and acrolein in the presence of  $BH_3$  and  $BF_3$  catalysts. The ab initio (HF/6-31++G\*\*) study of Tanaka and Kanemasa<sup>7</sup> showed that the nitron cycloaddition reaction with electron-deficient alkenes may occur through a stepwise mechanism when catalyzed by a strong Lewis acid. Roberson et al.<sup>8</sup> have also studied the mechanism of hetero-Diels–Alder reactions catalyzed by chiral aluminum

**Keywords:** AM1 theoretical study; Diels–Alder reaction;  $Zn^{2+}$  Lewis acid catalyst.

\* Corresponding author. Tel.: +55-162-739-964; fax: +55-162-739-975; e-mail: alberico@iqsc.sc.usp.br

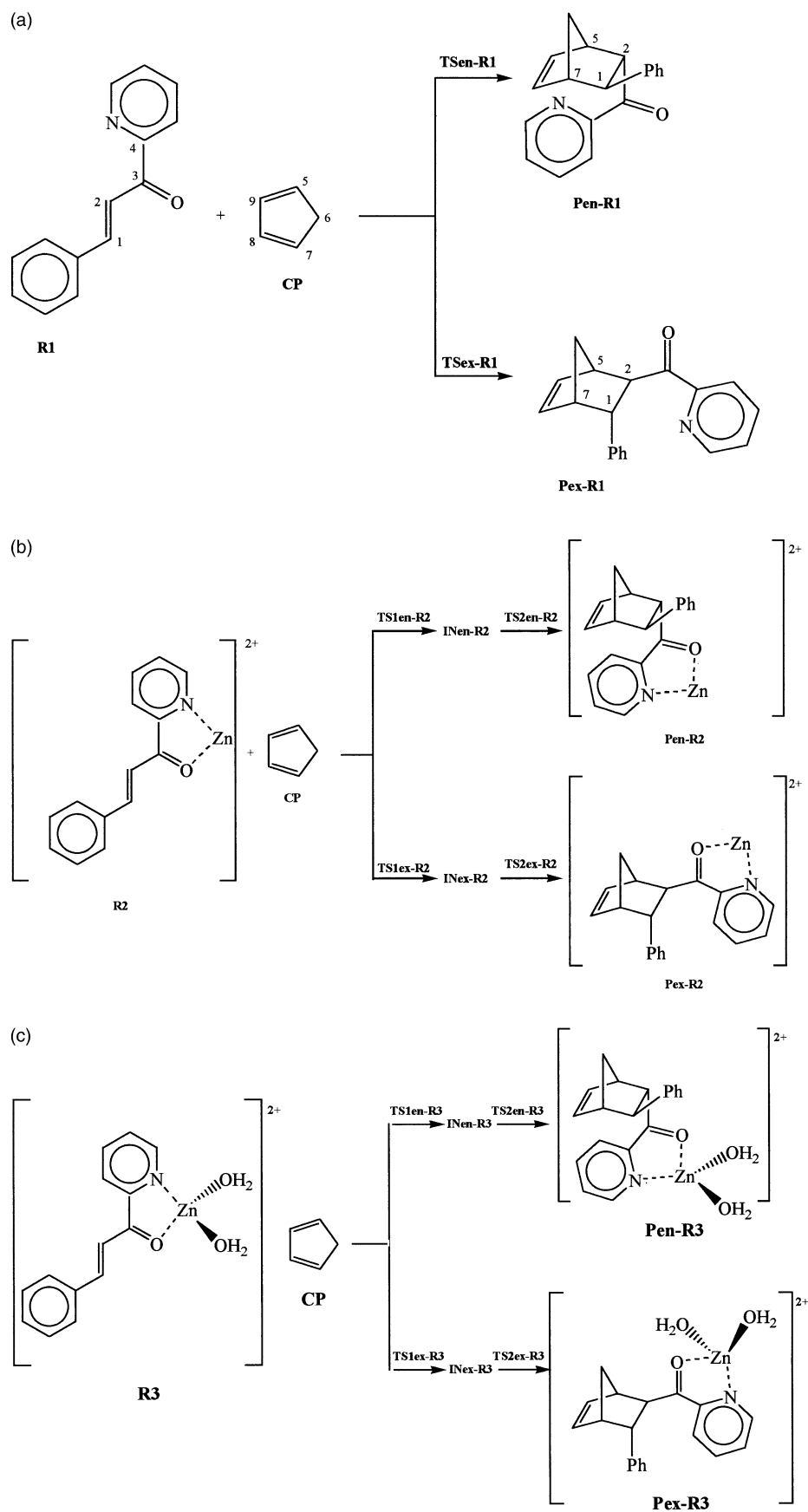


**Figure 1.** A representation of the Diels–Alder reaction (atom numbering included) between 3-phenyl-1-(2-pyridyl)-2-propen-1-one (R1) and cyclopentadiene (CP): (a) uncatalyzed process (R1+CP); (b)  $\text{Zn}^{2+}$  catalyzed process (R2+CP); (c)  $\text{Zn}(\text{H}_2\text{O})_2^{2+}$  catalyzed process (R3+CP).

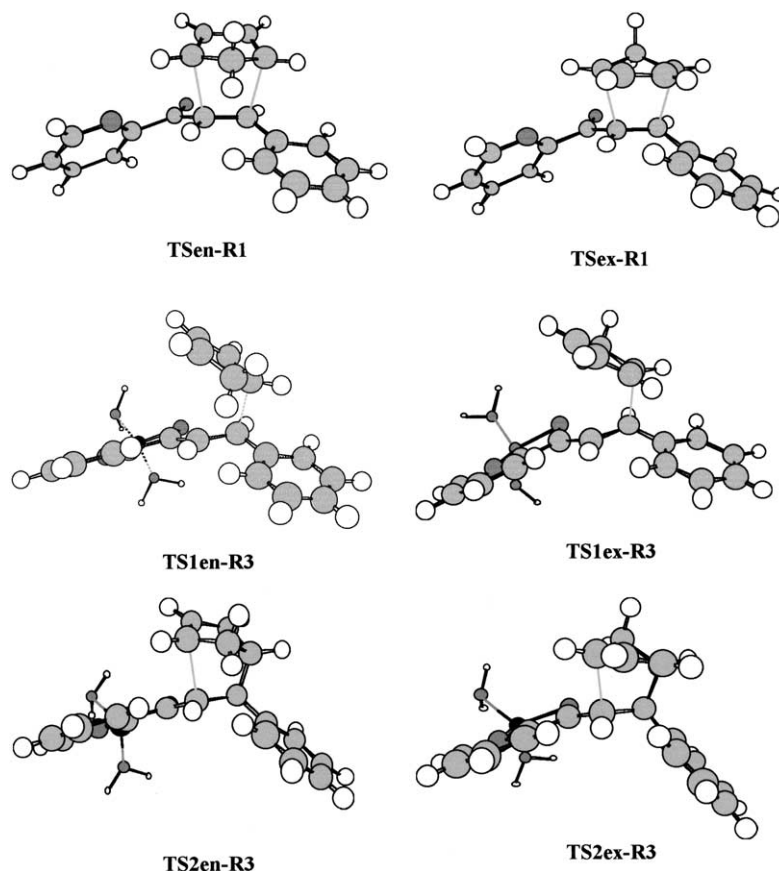


**Figure 2.** Transition structures corresponding to the uncatalyzed and catalyzed reactions between CP+R1 and CP+R3.

complexes. In that work, semiempirical (AM1) and ab initio (HF/6-31G<sup>\*</sup>) calculations<sup>8</sup> showed that the catalyzed reaction takes place through a stepwise mechanism.

This work presents a quantum chemical investigation of the effect of Zn<sup>2+</sup> Lewis acid catalyst on the mechanism of the Diels–Alder reaction between 3-phenyl-1-(2-pyridyl)-2-

propen-1-one (R1) and cyclopentadiene (CP). We performed a systematic AM1 semiempirical study with the aim to localize the stationary points for reactants, transition structures (TSs), products and possible intermediates on the potential energy surface (PES) for this cycloaddition.

The purpose of this work is to shed light on the mechanistic details of this important reaction. The Zn<sup>2+</sup> Lewis acid catalyst has been also included in order to clarify its role on the nature of the mechanism.

Here we would like to stress that the present investigation deals with trends rather than absolute values since full accurate results could not be expected from the AM1 semiempirical approach. However, this method may still be useful to investigate general trends and may help to elucidate the main factors responsible for the observed experimental outcomes. In fact, the elucidation of such factors are fundamental to a detailed understanding of the chemical reactivity and they are desired before embarking on more elaborate theoretical treatments.

## 2. Methods, computational procedures and models

Owing to the large size of the molecular systems studied in this work, ab initio calculations would be still expensive. On the other hand, semiempirical methods have recently progressed over the past few years to a surprising level of accuracy and reliability considering the limitations of the

**Table 1.** AM1 relative energies (kcal mol<sup>-1</sup>) to reactants for the stationary points of the reactions. AM1 heats of formation (kcal mol<sup>-1</sup>) for the reactants are: CP+R1=81.45; CP+R2=543.45; CP+R3=376.39

Stationary points	Relative energies (kcal mol <sup>-1</sup> )
TSen-R1	40.64
TSex-R1	39.39
Pen-R1	-13.18
Pex-R1	-6.22
TS1en-R2	5.14
TS1ex-R2	4.57
INen-R2	-17.27
INex-R2	-17.83
TS2en-R2	13.33
TS2ex-R2	12.22
Pen-R2	6.93
Pex-R2	6.91
TS1en-R3	11.60
TS1ex-R3	10.95
INen-R3	-6.39
INex-R3	-6.78
TS2en-R3	11.68
TS2ex-R3	10.17
Pen-R3	-1.76
Pex-R3	-1.67

underlying approximations.<sup>9,10</sup> Recently Roberson et al.<sup>8</sup> studied catalytic Diels–Alder reactions and showed that the AM1 semiempirical method predicted the same reaction course as predicted by an ab initio method (HF/6-31G).

In this work, AM1<sup>11</sup> semiempirical calculations were carried out using the AMPAC 6.0 program.<sup>12</sup> The PESs were calculated in detail to ensure that all relevant stationary points have been located and properly characterized. The stationary points on the PES were characterized by frequency calculations and the exact characterization of the TSs was achieved using a simple algorithm developed by us.<sup>13–15</sup> The optimization was carried out using the eigenvalue following routine<sup>16</sup> and the Berny analytical gradient optimization method.<sup>17,18</sup> Finally, the nature of each stationary point was determined by calculating analytically and diagonalizing the matrix of the energy second derivatives with the aim to determine the number of imaginary frequencies (zero for a local minimum and one for a TS).

The transition vector (TV),<sup>19</sup> i.e. the eigenvector associated to the unique negative eigenvalue of the force constant matrix, was also characterized and in order to verify that each saddle point leads to two putative minima, the intrinsic reaction coordinate (IRC) pathways from the TSs of the two lower energy structures were traced by using the second order Gonzalez and Schlegel interaction method.<sup>20,21</sup>

Fig. 1 shows the three selected models for this study. The first one corresponds to the uncatalyzed reaction between R1 and CP in the gas phase. The influence of the Lewis acid catalyst was modeled taking into account the formation of a complex between the carbonyl oxygen atom and the pyridyl nitrogen atom of R1 and Zn<sup>2+</sup> without molecules of water around the cation (second model-R2) and with the presence of two molecules of water around the cation (third model-R3).

As the dienophile (R1) can take two different conformations (*s-cis* or *s-trans*), which may bind with the diene (CP) and produce TSs in two possible conformations (*endo* or *exo*), we have considered in this work only the *s-cis* approach as previous ab initio<sup>22</sup> and DFT<sup>23</sup> calculations showed that the *s-cis* transition structure corresponds to the lowest energy in several Diels–Alder reactions.

### 3. Results and discussion

#### 3.1. Energies and geometries of stationary points

An exhaustive exploration of the PES for the [4+2] cycloaddition between R1 and CP affords that the reaction takes place along a concerted mechanism through two reactive channels (*endo* and *exo*). We have found two TSs, TSen-R1 and TSex-R1, and two cycloadducts, Pen-R1 and Pex-R1, corresponding to the *endo* and *exo* approaches, respectively (see Fig. 2 and Table 1). The relative energies of the stationary points along the different reaction pathways are showed in Table 1.

The energy barriers associated with the TSen-R1 and TSex-R1 processes are 40.64 and 39.39 kcal mol<sup>-1</sup>, respectively.

**Table 2.** Selected geometrical parameters (distances in Å and angles in degrees) and asynchronicity ( $\Delta r$ ) for the TSs

	C1–C7	C2–C5	O–C3–C4–N	$\Delta r$
TSen-R1	2.078	2.370	–141.75	0.29
TSex-R1	2.106	2.366	–137.31	0.26
TS1en-R2	2.127	3.619	14.16	1.49
TS1ex-R2	2.104	3.606	16.91	1.50
TS2en-R2	1.561	1.931	6.49	0.37
TS2ex-R2	1.556	1.914	5.61	0.36
TS1en-R3	2.034	3.587	13.61	1.55
TS1ex-R3	2.035	3.577	16.64	1.54
TS2en-R3	1.563	2.089	11.27	0.53
TS2ex-R3	1.559	2.062	10.22	0.50

The exothermic formation energies for the cycloadducts Pen-R1 and Pex-R1 are –13.18 and –6.22 kcal mol<sup>-1</sup>, respectively. Thus, owing to the small difference between the energy barriers, it is not possible to distinguish between the two transition states (TSen-R1 and TSex-R1) on the basis of the present calculations.

The TVs are dominated by the motion of the new (forming) C–C bonds and the extent of the asynchronicity ( $\Delta r$ ) can be measured by means of the difference between the distances of the bonds that are being formed in the reaction, i.e.  $\Delta r = d(C2-C5) - d(C1-C7)$  at TSen-R1 and TSex-R1. The corresponding  $\Delta r$  values for TSen-R1 and TSex-R1 are 0.29 and 0.26, respectively (see Table 2). The selected geometrical parameters for the different TSs are showed in Table 2. These results suggest that an asynchronous concerted mechanism should occur.

With the Zn<sup>2+</sup> Lewis acid in the R2 and R3 models, the cycloaddition most likely occurs through a stepwise mechanism. Four transition states and two intermediates have been found corresponding to the *endo* and *exo* approaches of CP towards R2 and R3. For these catalyzed reactions we have labeled the transition structures as TS1en-R2, TS1ex-R2, TS2en-R2, TS2ex-R2, TS1en-R3, TS1ex-R3, TS2en-R3 and TS2ex-R3. From these TSs, the related minima corresponding to the intermediates and the final cycloadducts were labeled as INen-R2, INex-R2, INen-R3 and INex-R3 and Pen-R2, Pex-R2, Pen-R3 and Pex-R3, respectively (see Fig. 1(b) and (c)).

The first step of the [4+2] cycloaddition corresponds to the nucleophilic attack of C7 carbon atom of CP to the C1 conjugated position of the R2 and R3 models with formation of the corresponding intermediate (IN). The second step corresponds to the ring closure of these intermediates to give the final cycloadducts achieved by the nucleophilic attack of the C2 position of R2 and R3 to the allyl C5 position of the CP moiety.

In the first step, the inclusion of the Zn<sup>2+</sup> Lewis acid decreases drastically the energy barrier associated with the carbon–carbon bond formation when compared to the concerted process. A comparison between the relative energies for the stationary points along the reaction of CP with R2 and R3 indicates that the TSs for the first step for R2 presents a lower energy barrier than for R3 while an opposite effect is found for the second step. The INex-R2 and INen-R2 intermediates are more stable than the

**Table 3.** Dipole moment ( $\mu$ ), in Debye, and charge transfer ( $Q^T$ ), in a.u., obtained with the Mulliken population analysis for the TSs of the Diels–Alder reactions studied

	$\mu$	$Q^T$
TSen-R1	3.61	0.14
TSex-R1	2.24	0.11
TS1en-R2	8.30	0.39
TS1ex-R2	7.19	0.33
TS2en-R2	15.17	0.51
TS2ex-R2	13.63	0.53
TS1en-R3	9.55	0.43
TS1ex-R3	9.98	0.42
TS2en-R3	14.16	0.53
TS2ex-R3	15.55	0.56

corresponding INex-R3 and INen-R3. This result can be ascribed to the fact that in the R2 model the  $Zn^{2+}$  cation retains to a larger extent the Lewis acidity of the bare ion owing to the absence of water molecules in its coordination sphere.

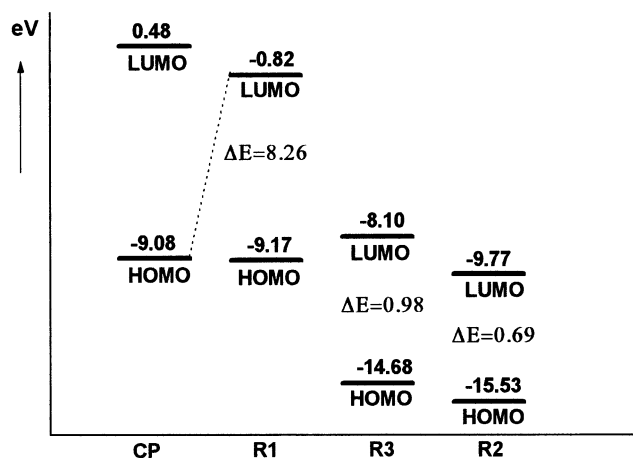
In fact since in the second step the TSs for R3 present a lower energy barrier than for R2, we can conclude that the R3 model (catalyst with molecules of water) is better than the R2 model (catalyst without molecules of water). Also, the R3 model is more realistic than the R2 one as it gives the correct number of coordination expected to the Zinc atom, i.e. four.

The length of the C1–C7 forming bonds for the R2 and R3 models in the TSs of the first step are in the range of 2.034–2.127 Å while the distance C2–C5 is in the range of 3.587–3.619 Å. The C2 and C5 atoms are not bonded along the first step and only the C1–C7 bonds are formed due to the nucleophilic attack of CP to the  $\beta$  position of the coordinated unsaturated ketone. Both C1 and C7 atoms are completely pyramidalized and the C8, C9 and C5 atoms have a planar disposition in agreement with a  $sp^2$  hybridization. This corresponds to an allylic arrangement of these three carbon atoms which allows a stabilization of the positive charge that is being developed along the nucleophilic attack of CP to the unsaturated ketone. The length of the C2–C5 forming bonds for the R2 and R3 models in the TSs of the second step are in the range of 1.914–2.089 Å. The TVs of the TSs of the first and second steps are associated to the C1–C7 and C2–C5 forming bonds, respectively.

### 3.2. Mulliken population analysis

A Mulliken population analysis allows us to evaluate the charge transfer process along the pathways of the cycloaddition reactions. The low values found for the charge transfer at the TSs corresponding to the uncatalyzed process (around 0.1 a.u., see Table 3) are in agreement with a bond-formation along the pericyclic process with a low polar character.

The charge transfer from the CP to the unsaturated ketone R2/R3 at the stepwise processes are: 0.4 a.u. (for the TSs of the first step), 0.6 a.u. (for INs) and 0.5 a.u. (for the TSs of the second step). These values indicate an increase of the charge transfer along the nucleophilic attack of CP to the electron-poor coordinated dienophile leading to the forma-

**Figure 3.** Energy of the frontier molecular orbitals for the cycloaddition reactions between CP and R1, R2 and R3.

tion of intermediates since the cyclopentadiene fragment supports an appreciable positive charge. Therefore, the role of the Lewis acid catalyst can be understood as an increase of the electrophilic character of the R1 system due to a stabilization of the corresponding TS through a delocalization of the negative charge that is being transferred along the nucleophilic attack by CP. This fact is responsible for the change of the mechanism in the catalyzed processes which are accomplished by a lowering of the energy barriers.

The uncatalyzed reaction, CP+R1, takes place along the pericyclic process with a large value for the energy barrier while the catalyzed reactions, CP+R2 or CP+R3, correspond to an ionic process initialized by the nucleophilic attack of CP to the unsaturated ketones that are coordinated to the Lewis acid. Therefore, CP and R2/R3 act as nucleophile and electrophile rather than diene and dienophile, respectively.

Also from Table 3 we can see that the charge transfer values obtained for the R3 model is slightly higher than for the R2 one. This shows that the solvent (the molecules of water added) has basically no influence in the charge transfer process.

### 3.3. Frontier molecular orbital analysis

The reactions studied in this work can be also understood through the frontier molecular orbital (FMO) model. The FMO model can be appropriate to explain the observed Lewis acid effects.<sup>24</sup> The role of the catalyst can be rationalized from Fig. 3 which shows that for the uncatalyzed process (CP+R1) the main HOMO–LUMO interaction occurs between the HOMO of the diene ( $HOMO_{CP}$ ) and the LUMO of the dienophile ( $LUMO_{R1}$ ). The  $LUMO_{R1}$  exhibits a relatively high energy and this is consistent with the large energy barrier found for the uncatalyzed process. However, when the oxygen and nitrogen atoms of the carbonyl group and pyridine fragment of R1 are coordinated to the  $Zn^{2+}$  (R2 and R3 models) both HOMO and LUMO energies of R1 decrease considerably. This effect, that is consonant with the high stabilization of

the TSs, decreases the energy difference between HOMO<sub>CP</sub> and LUMO<sub>R2/R3</sub> and is responsible for the increase of the reaction rate. Our FMO calculations showed that the calculated frontier orbital energies are in qualitative agreement with the experimental results.<sup>5b</sup>

#### 4. Conclusions

In this work we have carried out a theoretical study on the mechanism of the reaction between 3-phenyl-1-(2-pyridyl)-2-propen-1-one and cyclopentadiene, both in the absence and the presence of Zn<sup>2+</sup> acting as a Lewis acid, by using the AM1 semiempirical method.

The following conclusions can be drawn from the results obtained in this study:

- (i) the cycloaddition reaction between 3-phenyl-1-(2-pyridyl)-2-propen-1-one and cyclopentadiene takes place along an asynchronous concerted mechanism. Two reactive channels have been characterized corresponding to the *endo/exo* approaches;
- (ii) the coordination of the Zn<sup>2+</sup> cation to the carbonyl oxygen atom and the nitrogen atom of the pyridine ring of 3-phenyl-1-(2-pyridyl)-2-propen-1-one changes the mechanism from concerted to stepwise through two TSs and one intermediate. The reaction can be described as a nucleophilic attack of the cyclopentadiene to the  $\beta$  position of the  $\alpha,\beta$ -unsaturated ketone (with formation of the corresponding intermediate) followed by a ring closure process yielding the final cycloadduct;
- (iii) the bidentate 3-phenyl-1-(2-pyridyl)-2-propen-1-one (that is coordinated to the Zn<sup>2+</sup> Lewis acid) and the cyclopentadiene act as an electrophile and a nucleophile, respectively;
- (iv) The AM1 semiempirical calculations with the Zn<sup>2+</sup> Lewis acid showed that the reaction pathways take place through a stepwise mechanism (with a very low energy barrier) causing a lowering of the LUMO energy and consequently having a smaller HOMO–LUMO gap. Due to these effects, a faster reaction takes place in the presence of such metal ion.

#### Acknowledgements

This work was supported by the Programa de Colaboración Científica con Iberoamérica (Proyecto 8i051). Calculations were performed on a Silicon Graphics Octane R12000 workstation of the Departament de Ciències Experimentals and on two Silicon Graphics Power Challenger L of the Servei d'Informàtica of the Universitat Jaume I. We are indebted to these centers for providing us with computer capabilities. M. O. thanks the Universitat Jaume I for a FPI fellowship. S. M. thanks Generalitat Valenciana for a doctoral grant. C. N. Alves and A. B. F. da Silva would like to thank the Brazilian agencies CAPES and CNPq for the financial support.

#### References

1. (a) Oppolzer, W. *Angew. Chem., Int. Ed. Engl.* **1984**, *33*, 497. (b) Carruthers, W. *Cycloaddition Reaction in Organic Synthesis*; Pergamon: Oxford, 1990. (c) Ressig, H.-U. *Organic Synthesis Highlights*; VCH: Weinheim, 1991 p 71. (d) Kagan, H. B.; Riant, O. *Chem. Rev.* **1992**, *92*, 1007. (e) Stipanovic, R. D. *Environ. Sci. Res.* **1992**, *44*, 319. (f) Pindur, U.; Lutz, G.; Otto, C. *Chem. Rev.* **1993**, *93*, 741. (g) Li, C.-J. *Chem. Rev.* **1993**, *93*, 2023. (h) Togni, A.; Venanzi, L. M. *Angew. Chem., Int. Ed. Engl.* **1994**, *33*, 497. (i) Cativiela, C.; Garcia, J. I.; Mayoral, J. A.; Salvatella, L. *Chem. Soc. Rev.* **1996**, 209. (j) Laschat, S. *Angew. Chem., Int. Ed. Engl.* **1996**, *35*, 289. (k) Kumar, A. *Chem. Rev.* **2001**, *101*, 1. (l) Fringuelli, F.; Piermatti, O.; Pizzo, F.; Vaccaro, L. *Eur. J. Org. Chem.* **2001**, 439.
2. Yates, P.; Eaton, P. *J. Am. Chem. Soc.* **1960**, *82*, 4436.
3. (a) Fringuelli, F.; Taticchi, A.; Wenkert, E. *Org. Prep. Proced. Int.* **1990**, *22*, 131. (b) Fringuelli, F.; Minuti, L.; Pizzo, F.; Taticchi, A. *Acta Chem. Scand.* **1993**, *47*, 255.
4. Bosnich, B. *Aldrichimica Acta* **1998**, *31*, 76.
5. (a) Otto, S.; Engberts, J. B. F. N. *Tetrahedron Lett.* **1995**, *36*, 2645. (b) Otto, S.; Bertoncin, F.; Engberts, J. B. F. N. *J. Am. Chem. Soc.* **1996**, *118*, 7702. (c) Otto, S.; Engberts, J. B. F. N. *J. Am. Chem. Soc.* **1998**, *120*, 9517.
6. Alves, C. N.; Camilo, F. F.; Gruber, J.; Da Silva, A. B. F. *Tetrahedron* **2001**, *57*, 6877.
7. Tanaka, J.; Kanemasa, S. *Tetrahedron* **2001**, *57*, 899.
8. Roberson, M.; Jepsen, A. S. J.; Jorgensen, K. A. *Tetrahedron* **2001**, *57*, 907.
9. Stewart, N. C. *Semiempirical Molecular Orbitals Methods*; Wiley: New York, 1990.
10. Zerner, M. C. *Semiempirical Molecular Orbitals Methods*; Wiley: New York, 1991.
11. Dewar, M. J. S.; Zoebisch, E. G.; Healy, E. F.; Stewart, J. J. P. *J. Am. Chem. Soc.* **1985**, *107*, 3902.
12. *AMPAC 6.0 User's Manual*; Semichem: Shawnee, 1997.
13. Tapia, O.; Andrés, J. *J. Chem. Phys. Lett.* **1984**, *109*, 471.
14. Andrés, J.; Moliner, V.; Safont, V. S. *J. Chem. Soc., Faraday Trans.* **1994**, *90*, 1703.
15. Tapia, O.; Andrés, J.; Safont, V. S. *J. Chem. Soc., Faraday Trans.* **1994**, *90*, 2365.
16. Baker, J. J. *Comp. Chem.* **1986**, *7*, 385.
17. Schlegel, H. B. *J. Comp. Chem.* **1982**, *3*, 214.
18. Schlegel, H. B. *J. Chem. Phys.* **1982**, *77*, 3676.
19. McIver, J. W. *J. Acc. Chem. Res.* **1974**, *7*, 72.
20. González, C.; Schlegel, H. B. *J. Phys. Chem.* **1990**, *94*, 5523.
21. González, C.; Schlegel, H. B. *J. Chem. Phys.* **1991**, *95*, 5853.
22. Jorgensen, W. L.; Lim, D.; Blake, J. F. *J. Am. Chem. Soc.* **1993**, *115*, 2936.
23. García, J. I.; Martínez-Merino, V.; Mayoral, J. A.; Salvatella, L. *J. Am. Chem. Soc.* **1998**, *120*, 2415.
24. Fleming, I. *Frontier Orbitals and Organic Chemical Reactions*; Wiley: Chichester, 1996.